BIOCHEMISTRY
including biophysical chemistry & molecular biology

ARTICLE

pubs.acs.org/biochemistry

The L76V Drug Resistance Mutation Decreases the Dimer Stability and Rate of Autoprocessing of HIV-1 Protease by Reducing Internal Hydrophobic Contacts

John M. Louis,[*,†] Ying Zhang,[‡] Jane M. Sayer,[†] Yuan-Fang Wang,[§] Robert W. Harrison,[§,∥] and Irene T. Weber[*,‡,§]

[†]Laboratory of Chemical Physics, National Institute of Diabetes and Digestive and Kidney Diseases, National Institutes of Health, Bethesda, Maryland 20892, United States

[‡]Department of Chemistry, Molecular Basis of Disease Program, Georgia State University, Atlanta, Georgia 30303, United States

[§]Department of Biology, Molecular Basis of Disease Program, Georgia State University, Atlanta, Georgia 30303, United States

[∥]Department of Computer Science, Molecular Basis of Disease Program, Georgia State University, Atlanta, Georgia 30303, United States

ABSTRACT: The mature HIV-1 protease (PR) bearing the L76V drug resistance mutation (PR_{L76V}) is significantly less stable, with a >7-fold higher dimer dissociation constant (K_d) of 71 ± 24 nM and twice the sensitivity to urea denaturation (UC_{50} = 0.85 M) relative to those of PR. Differential scanning calorimetry showed decreases in T_m of 12 °C for PR_{L76V} in the absence of inhibitors and 5−7 °C in the presence of inhibitors darunavir (DRV), saquinavir (SQV), and lopinavir (LPV), relative to that of PR. Isothermal titration calorimetry gave a ligand dissociation constant of 0.8 nM for DRV, ∼160-fold higher than that of PR, consistent with DRV resistance. Crystal structures of PR_{L76V} in complexes with DRV and SQV were determined at resolutions of 1.45−1.46 Å. Compared to the corresponding PR complexes, the mutated Val76 lacks hydrophobic interactions with Asp30, Lys45, Ile47, and Thr74 and exhibits closer interactions with Val32 and Val56. The bound DRV lacks one hydrogen bond with the main chain of Asp30 in PR_{L76V} relative to PR, possibly accounting for the resistance to DRV. SQV shows slightly improved polar interactions with PR_{L76V} compared to those with PR. Although the L76V mutation significantly slows the N-terminal autoprocessing of the precursor TFR-PR_{L76V} to give rise to the mature PR_{L76V}, the coselected M46I mutation counteracts the effect by enhancing this rate but renders the TFR-$PR_{M46I/L76V}$ precursor less responsive to inhibition by 6 μM LPV while preserving inhibition by SQV and DRV. The correlation of lowered stability, higher K_d, and impaired autoprocessing with reduced internal hydrophobic contacts suggests a novel molecular mechanism for drug resistance.

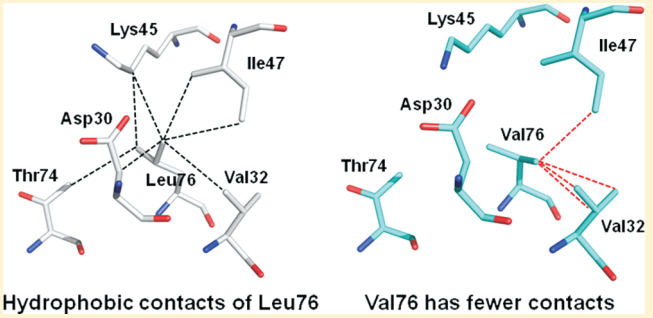

Human immunodeficiency HIV-1 protease (PR) is a major drug target for the treatment of AIDS. PR functions in the last step of the HIV-1 life cycle by catalyzing the cleavage of viral polyproteins produced in the host cell.[1] Hydrolysis of polyproteins into functional products is important for the maturation and production of infectious progeny virions. Protease inhibitors (PIs) act to prevent the maturation process. Currently, nine PIs are approved by the Food and Drug Administration as antiviral drugs. However, the lack of a proofreading step of the viral reverse transcription leads to a high frequency of mutations, and under drug pressure, rapid selection of a combination of mutations confers drug resistance, thus presenting a severe challenge in current anti-HIV treatment.[2]

PR is a homodimer with 99 amino acids in each subunit (Figure 1).[3] The Asp25-Thr26-Gly27 triplets of both monomers form the catalytic site, where Asp25 and Asp25′ (the prime indicates the second subunit of the dimer) serve as general acid−base catalysts of polyprotein cleavage in the proposed reaction mechanism.[4] Two flexible interacting flaps are formed by residues 44−57 of both subunits. The two characteristic triplets and two flaps make important contributions to the active site cavity for the binding of substrates or inhibitors.[5] The PR dimer is stabilized via noncovalent interactions of the residues at the dimer interface. Important intersubunit hydrogen bonds connect the catalytic triplets, flaps, and β-sheet formed by the four terminal strands.[6] The tertiary fold of each monomer is stabilized by hydrophobic interactions among the aliphatic residues in an internal hydrophobic core. Mutations occurring in more than 30 of the 99 residues in each subunit are associated with drug resistance.[7] Two major types of PI resistance mutations are proposed to influence the PR activity.[5] One type located near the active site can change the binding affinity and/or

Received: January 7, 2011
Revised: March 1, 2011
Published: March 29, 2011

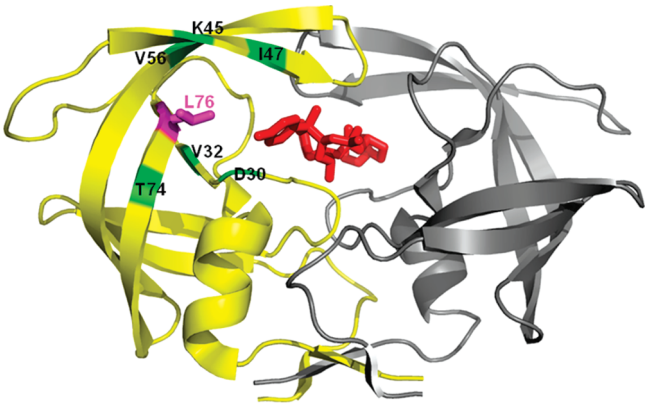

Figure 1. HIV-1 PR dimer structure (gray and yellow ribbons represent the two subunits) bound to darunavir (red sticks). The site of mutation is shown with magenta sticks for Leu76 on one subunit. Positions of residues interacting with Leu76 are labeled and colored green.

specificity of PR with the inhibitor by altering direct interactions.[8] Other mutations do not change the binding cavity directly; however, they may affect PR stability and indirectly influence the binding of inhibitors via long-range structural perturbations.[9]

The L76V mutation has become more prevalent in data sets of HIV-1 mutants observed in patients.[7] The presence of the L76V mutation as a single mutation was shown to hamper viral replication severely.[10] The L76V mutation, generally accompanied by other mutations, is considered a major mutation providing 2−6-fold decreased susceptibility to darunavir (DRV), fosamprenavir, indinavir (IDV), and lopinavir (LPV).[11,12] It is also selected as a drug resistance mutation in patients receiving LPV therapy.[10] This mutation, however, is not associated with resistance to atazanavir (ATV), nelfinavir (NFV), saquinavir (SQV), or tipranavir (TPV). Instead, mutants containing L76V exhibit increased susceptibility to these drugs.[11,13,14] Hence, this mutation shows opposing roles in drug resistance, acting to increase susceptibility to some drugs and decrease susceptibility to others.[15]

We constructed PR with the single L76V mutation to investigate its effect on the structure, stability, and activity of the enzyme. Crystal structures of PR_{L76V} with DRV and SQV were determined to investigate the molecular basis for the responses of this mutant to inhibitors. Leu76 is located in the hydrophobic core of PR close to the active site cavity, although its side chain has no van der Waals contacts with most substrates or inhibitors. Additionally, the effect of the mutation on the autocatalytic processing of the precursor, which is required for the onset of the catalytic activity characteristic of the mature, dimeric enzyme, was assessed in vitro, and the effect of a second mutation, M46I, was examined in the precursor containing both mutations.

EXPERIMENTAL PROCEDURES

Protein Expression and Purification. The HIV-1 PR (GenBank entry HIVHXB2CG) clone optimized for structural and biochemical studies contains Q7K, L33I, and L63I mutations to minimize autoproteolysis and C67A and C95A mutations to prevent cysteine-thiol oxidation.[16] The L76V mutation was introduced into this PR template as well as the template encoding a PR precursor mimetic in which the full-length transframe region (TFR) is fused to the N-terminus of PR (TFR-PR) by use of the appropriate oligonucleotide primers using the QuikChange protocol (Stratagene, La Jolla, CA) and verified by DNA sequencing. A second construct, containing two mutations, M46I and L76V, in the PR domain of TFR-PR was also made using $TFR\text{-}PR_{L76V}$ as the template. Proteins were expressed using the pET11a vector and *Escherichia coli* BL21(DE3) cells, purified, and refolded using established protocols,[17−19] and the identities of the products were verified by ESI-MS.

Enzyme Assays. The kinetic parameters were measured using a fluorescence assay as described previously[20] with the substrate Abz-Thr-Ile-Nle-pNO_2Phe-Gln-Arg-NH_2 (where pNO_2Phe is *p*-nitrophenylalanine, Nle is norleucine, and Abz is anthranilic acid) (Bachem Bioscience Inc., King of Prussia, PA), which is based on the p2/NC cleavage site of the viral polyprotein. PR_{L76V} (10 μL) at a final concentration of 34 nM from active site titration with SQV was mixed with 100 μL of reaction buffer [100 mM MES (4-morpholineethanesulfonic acid) (pH 5.6), 400 mM NaCl, 1 mM ethylenediaminetetraacetic acid, and 5% glycerol] at 26 °C. The reaction was initiated by addition of substrate from a 186 μM stock solution, yielding a final concentration of 12−84 μM. PR activity was measured by monitoring the increase in fluorescence over 5 min using an excitation wavelength of 340 nm and an emission wavelength of 420 nm (pNO_2Phe as the quencher (fluorescent acceptor) and Abz as the fluorescent donor) with a POLARstar OPTIMA 96-well microplate instrument (BMC Labtech). Values for k_{cat} and K_m were obtained by fitting the curves to the Michaelis−Menten equation using SigmaPlot (SPSS Inc., Chicago, IL).

For dimer dissociation and urea denaturation studies, enzyme activity was measured by following the initial rates of hydrolysis of the chromogenic peptide substrate IV that mimics the CA/p2 cleavage site (Lys-Ala-Arg-Val-Nle-pNO_2Phe-Glu-Ala-Nle-NH_2, California Peptide Research, Napa, CA) at 310 nm ($\Delta\varepsilon$ = 1797 M^{-1} cm^{-1}) in 50 mM sodium acetate buffer (pH 5.0) at 28 °C. The substrate concentration (390 μM in the assay mixtures) was determined from the UV spectrum of substrate stock solutions (ε_{280} = 12000 M^{-1} cm^{-1}). The dimer dissociation constant, K_d, was determined by fitting the curve of activity (initial rate/protease concentration) versus protease concentration (40−1200 nM as monomers) to an equation described previously.[19] For urea denaturation studies, activity was measured at urea concentrations of 0−3.5 M[16,21] and an enzyme concentration of 0.3−1.15 μM. The UC_{50} value is the urea concentration at which the PR activity is half of the maximal activity in the absence of urea.

Calorimetry. Inhibitor concentrations were determined kinetically by active site titration against the wild-type PR. Samples for differential scanning calorimetry (DSC) were prepared by the quench protocol from stock solutions in HCl as previously described,[18] giving a final enzyme concentration of 14−15 μM (as dimer) in 50 mM sodium acetate buffer (pH 5.0). Final concentrations of inhibitors DRV, SQV, and LPV were 28−29 μM (~2-fold molar excess relative to the dimeric enzyme). DSC scans were taken on a MicroCal VP-DSC microcalorimeter (GE Healthcare) at 90 °C/h from a starting temperature of 20 °C and terminated at 70−90 °C depending on the position of the transition. Data were processed using the instrument's Origin software as described previously.[22] Sodium dodecyl sulfate−polyacrylamide gel electrophoresis (SDS−PAGE) of the inhibitor-free enzyme on a 20% homogeneous PhastGel (GE Healthcare) before and after DSC showed no evidence of autoproteolysis during the course of the DSC experiment.

For isothermal titration calorimetry, PR_{L76V} (1.9 mg/mL in 12 mM HCl) was folded by the quench protocol[18] to give final concentrations of 8−13.5 μM in 50 mM sodium acetate buffer (pH 5) and titrated with 16 injections of DRV in the same buffer (60−140 μM depending on the protein concentration) by use of a MicroCal iTC_{200} microcalorimeter (GE Healthcare) at 28 °C. Stock 160−200 μM inhibitor solutions were prepared in low-ionic strength buffers at a final DMSO concentration of 0.5% (v/v), diluted from a stock solution of inhibitor in 100% DMSO. All ITC experiments were performed at DMSO concentrations of ≤0.5%. DMSO equivalent to that in the titrant was added to the protein solution in the cell to minimize thermal effects of changing DMSO concentration during the titration. As reduced autoproteolysis is intrinsic to the optimized PRs after folding at pH 5, concentrations of active PR_{L76V} were verified from the known stoichiometry of inhibitor binding to the active site (N = 1) upon titration. Data were processed using the instrument's Origin software. Three separate experiments at different concentrations of PR_{L76V} and DRV were consistent with an upper limit of ~10 nM for the dissociation constant (K_L). A displacement titration with 50 μM DRV in the presence of 16 μM RPB inhibitor [H-Arg-Val-Leu-(r)-Phe-Glu-Ala-Nle-NH_2, Bachem Americas, Inc., Torrance, CA] added to the sample cell containing 4 μM PR_{L76V} provided a more accurate value. Analogous displacement titrations under the same conditions with SQV or LPV did not give an adequate thermal effect for reliable quantitation.

Autoprocessing of the TFR-PR_{L76V} Precursor. Isolation of PR precursors in significant quantities presents a substantial challenge because the intrinsic autoprocessing of the precursors to mature protease results in their depletion during expression. However, amounts of the full-length precursors sufficient for small scale experiments can be recovered. Thus, remnants of the unprocessed precursor TFR-PR_{L76V} and TFR-$PR_{M46I/L76V}$ were purified as described previously.[16,19] The precursor was folded by addition of 5.66 volumes of 5 mM sodium acetate buffer (pH 5.3), with or without added DRV, to TFR-PR_{L76V} in 12 mM HCl, to give a final pH of 4.5. Samples (5 μL) were removed at times from 0 to 26 h, mixed with 3 μL of SDS−PAGE sample buffer, and frozen immediately. Samples were subjected to electrophoresis on 20% homogeneous PhastGels (GE Healthcare) and visualized by staining with PhastGel Blue R.

Crystallographic Analysis. PR_{L76V} at a concentration of 7 mg/mL was mixed with DRV or SQV at a 5-fold molar excess. Crystals were grown by the hanging-drop vapor-diffusion method at room temperature using 24-well VDX plates (Hampton Research, Aliso Viejo, CA). The crystallization drops had equal volumes of the protein and reservoir solutions. Crystals of PR_{L76V} with DRV grew in solutions of 30 mM NaOAc buffer (pH 4.6−5.0), 1.4−1.8 M NaCl, and 3% (v/v) DMSO. Crystals of PR_{L76V} with SQV grew in solutions of 100 mM Tris-HCl buffer (pH 6.0−9.0) and 1.3 M NaCl with 3% (v/v) DMSO. The crystals were frozen in liquid nitrogen with a cryoprotectant of 20−30% (v/v) glycerol. X-ray diffraction data for the crystals were collected on beamline SER-CAT of the Advanced Photon Source (Argonne National Laboratory, Argonne, IL).

X-ray data were processed with HKL2000.[23] The structures were determined by molecular replacement using MolRep in the CPP4i suite of programs,[24] and the starting model was the wild-type PR complex with DRV [Protein Data Bank (PDB) entry 2IEN][25] in the same space group as the new structures. The structures were refined with SHELXL[26] and refitted using Coot 0.3.3.[27] Alternate conformations were modeled for PR residues, inhibitors, and solvent molecules based on the observed electron density maps. The solvent was modeled with more than 200 water molecules, ions, and other solvent molecules present in the crystallization solutions, as described previously.[25] Anisotropic B factors were applied for all the structures. Hydrogen atom positions were calculated in the last stage of refinement, using all data once all other parameters, including disorder, had been modeled. The mutant crystal structures were compared with the wild-type PR by superimposing their C_α atoms as described previously.[25] Structural figures were made using PyMol.[28]

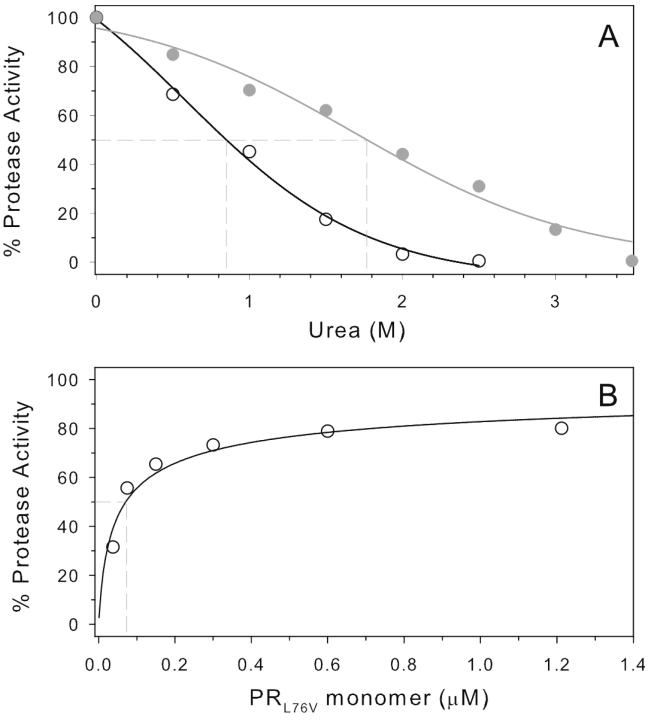

Figure 2. (A) Urea denaturation of PR_{L76V} and wild-type PR (UC_{50} = 0.85 and 1.78 M, respectively, dashed intersect on the X-axis). (B) Kinetic determination of PR_{L76V} dimer dissociation. A dissociation constant (K_d = 71 ± 24 nM), indicated by the dashed vertical line at 50% activity, was determined (see Experimental Procedures). For the wild-type PR, the K_d is <10 nM (not shown; ref 29).

Protein Data Bank Entries. The structure coordinates and factors have been deposited in the RCSB Protein Data Bank as entries 3PWM for the PR_{L76V}−DRV complex and 3PWR for the PR_{L76V}−SQV complex.

RESULTS AND DISCUSSION

Properties and Stability of Mature PR_{L76V}. Purified mature PR_{L76V} exhibited a K_m of 37 ± 6 μM and a k_{cat} of 334 ± 23 min^{-1} at pH 5.6 and 200 mM NaCl. The catalytic efficiency, k_{cat}/K_m, of 9.0 μM^{-1} min^{-1} for hydrolysis of the fluorogenic substrate based on the p2/NC cleavage site is essentially the same (1.2-fold) as the value of 7.2 μM^{-1} min^{-1} determined for PR under the same conditions.[20] A plot of the dependence of activity on urea concentration (Figure 2A) shows a transition midpoint (UC_{50}) of 0.85 M urea for PR_{L76V}, which is approximately half the value of 1.78 M for PR (Table 1). Increased susceptibility to urea denaturation is consistent with the lower stability of the PR_{L76V} dimer relative to that of the wild-type enzyme as reflected by the

Table 1. Dimer Dissociation and Urea and Thermal Denaturation of PR_{L76V}

protease	UC_{50} (M)	K_d (nM)	T_m (°C) without inhibitor	T_m (ΔT_m) (°C) DRV	T_m (ΔT_m) (°C) SQV	T_m (ΔT_m) (°C) LPV
PR_{L76V}	0.85	71	53.7	80.9 (27.2)	79.5 (25.8)	79.1 (26.1)
PR	1.78	<10[a]	65.7[b]	88.1[b] (22.4)	85.0[b] (19.3)	not determined by DSC (20.4)[c]

[a] Data from ref 16. [b] Data from ref 30. [c] ThermoFluor data from ref 31.

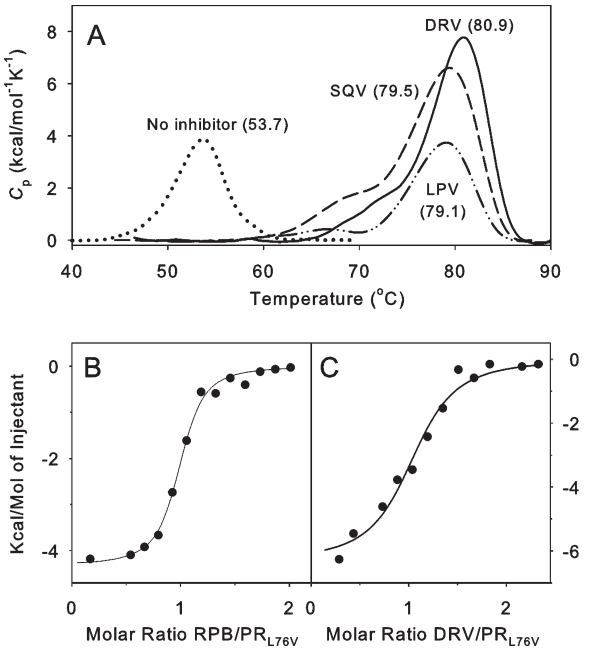

Figure 3. Thermochemical data for interactions of inhibitors with PR_{L76V}. (A) DSC thermograms of PR_{L76V} in the presence and absence of inhibitors in 50 mM sodium acetate buffer (pH 5.0). The thermal transition temperatures (curve maxima) are in parentheses. Inhibitors were in a 2-fold molar excess relative to dimeric PR_{L76V}. (B) ITC trace of 5 μM PR_{L76V} titrated with 80 μM RPB (K_L = 61 nM) in 50 mM sodium acetate buffer (pH 5). (C) Displacement of RPB (total concentration of 16 μM) bound to 4.2 μM PR_{L76V} by titration with DRV (50 μM; K_L for DRV = 0.79 nM).

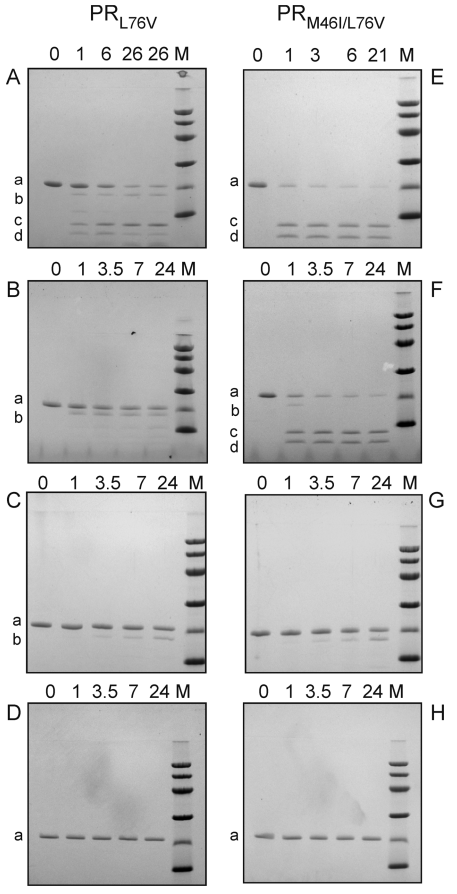

Figure 4. Autocatalytic maturation and inhibition of precursors (TFR-PR_{L76V} and TFR-$PR_{M46I/L76V}$) at pH 4.5. Inhibitors were present at a 1:1 molar ratio (6 μM) with respect to precursors (as dimers): (A and E) controls without inhibitor, (B and F) in the presence of LPV, (C and G) in the presence of SQV, and (D and H) in the presence of DRV. Numbers indicated above the gels denote autoprocessing reaction times in hours. Lane M corresponds to markers of 97, 66, 45, 30, 20, and 14 kDa from the top. Letter designations for the bands are as follows: a, full-length precursor; b, TFR^{9-56}-PR; c, mature, active PR; d, fragment TFR^{9-56}.

K_d of 71 ± 24 nM for PR_{L76V} (Figure 2B), which is at least 7-fold higher than that of PR.[29]

Inhibitor Binding. Differential scanning calorimetry (Figure 3A) was used to assess the thermal denaturation of PR_{L76V} in the absence and presence of inhibitors. The observed T_m values for PR_{L76V} in Table 1 are compared with those previously reported for PR under the same conditions.[30] In the absence of inhibitors, PR_{L76V} is markedly less stable to thermal denaturation, with a T_m that is 12 °C lower than that of PR. Although the mechanisms of heat- and urea-induced denaturations are not necessarily the same, the low T_m value for PR_{L76V} is consistent with the observed effect of urea on its catalytic activity, as both heat and urea denaturations involve changes in the stability of the protein fold, which may precede and/or accompany dimer dissociation. Even when the PR forms complexes with inhibitors, which should stabilize the proteases as dimers, the T_m value for PR_{L76V} is ~7 °C lower than that for PR. The decreased thermal stability of PR_{L76V} contrasts with results reported for several other PR mutants associated with drug resistance. For example, T_m values for ATV resistant mutant I50L/A71V[31] and multidrug resistant mutant V82F/I84V[32] were both higher than the values observed for PR by 2.2 and 4 °C, respectively. A multidrug resistant mutant bearing 11 mutations also exhibited a slightly higher T_m than the wild-type enzyme.[33]

An upper limit of ~10 nM for the dissociation constant (K_L) of the PR_{L76V}—DRV complex, with a range between 6.6 and 18 nM, was obtained by direct ITC titrations with the inhibitor. A substrate analog inhibitor (RPB) with a reduced peptide bond exhibits a good negative thermal response (ΔH = −4.3 kcal/mol)

upon binding to PR_{L76V} and a K_L of 61 ± 13 nM (Figure 3B). A displacement titration with DRV in the presence of RPB gave a value of 0.79 ± 0.29 nM (Figure 3C), approximately 160-fold larger than K_L for the PR−DRV complex.[34,35] The lack of an adequate thermal response under the same conditions, either upon direct titration or via displacement of RPB (10−15 μM), precluded K_L measurements with SQV and LPV. Alternatively, a qualitative indication of the relative binding affinity of different inhibitors to the same protein can be obtained from the increase in the thermal denaturation temperature (ΔT_m) in the presence of an inhibitor.[22,30,31] The values of ΔT_m for binding of DRV, SQV, and LPV to PR_{L76V} are significantly larger (by 5−7 °C) than those for binding to PR, reflecting both the low thermal stability of the free PR_{L76V} and significant stabilization of the protein−inhibitor complexes. ΔT_m values for binding of DRV, SQV, and LPV to PR_{L76V} (Figure 3A) differ by less than 2 °C in the order DRV > SQV > LPV and are consistent with large binding constants (small K_L values), although their enthalpy values for thermal denaturation decrease significantly in the same order. The effects of these three inhibitors on autoprocessing of the TFR-PR_{L76V} precursor (cf. Figure 4 and the following section) suggest that K_L values for SQV and LPV will be larger than the value of 0.8 nM observed by ITC for DRV. By contrast, in vitro phenotype assays found the L76V mutation in PR derived from clinical samples is associated with enhanced susceptibility to SQV and resistance to DRV and LPV.[11,14] However, in many, if not most, DRV resistant clinical isolates, a single resistance mutation does not occur alone but is associated with other mutations such as M46I and L90M,[13,36] which are selected along with the L76V mutation in clinical settings. It is possible that the relative responses to these inhibitors as well as the dimer stability are altered by the presence of such additional mutations.

Autoprocessing of PR_{L76V} and $PR_{M46I/L76V}$ Precursors. During viral replication, the autocatalytic processing (autoprocessing) of PR from its Gag-Pol polyprotein precursor is essential for generating the active mature PR and requisite structural and functional proteins of the infective virion.[3] Cleavage between the transframe region (TFR), encoded in the Pol open reading frame, and the N-terminus of the PR domain (TFR/PR site) is crucial for the formation of stable PR dimers with full catalytic activity from the monomeric TFR-PR. Consequently, compromising this process will adversely affect the viability of the virus. Previous studies with the wild-type precursor, TFR-PR, have identified the pathways for its maturation.[3,29] The time course of autoprocessing in the absence of inhibitors and in the presence of LPV, SQV, and DRV is shown in Figure 4. At low pH values, an initial cleavage of TFR-PR (a) occurs between F8 and L9 of the TFR to give an intermediate (b) with low catalytic activity similar to the full-length precursor. Subsequent cleavage at the TFR/PR site releases the fully active, mature PR (c) and the fragment TFR^{9-56} (d). Autoprocessing was assessed in vitro with a precursor comprising the 56-amino acid TFR fused to the N-terminus of the PR domain containing the L76V mutation (TFR-PR_{L76V}). Reactions conducted at ∼6 μM protein permit monitoring of the autoprocessing of the precursor in small volumes suitable for SDS−PAGE on PhastGels. In the absence of inhibitors, only ∼50% of the autoprocessing reaction is complete after 6 h (Figure 4A), in contrast to that of wild-type TFR-PR, which is complete in <1 h.[3,37] Thus, the slower rate of autoprocessing of TFR-PR_{L76V} seems to correlate with the lower stability of the mature PR_{L76V}, namely, the higher K_d and increased susceptibility to denaturation by urea.

Table 2. Crystallographic Data Collection and Refinement Statistics

protease	PR_{L76V}	PR_{L76V}
inhibitor	DRV	SQV
space group	$P2_12_12$	$P2_12_12$
unit cell dimensions (Å)		
a	58.32	58.84
b	86.33	86.17
c	45.98	46.24
resolution range (Å)	50−1.46	50−1.45
no. of unique reflections	37895	38308
R_{merge} (%) [overall (final shell)]	5.2 (49.2)	6.4 (48.0)
$\langle I/\sigma \rangle$ [overall (final shell)]	34.9 (2.1)	27.3 (2.2)
data range for refinement (Å)	10−1.46	10−1.45
completeness (%) [overall (final shell)]	91.9 (54.9)	90.1 (56.4)
R_{work}	0.1404	0.1449
R_{free}	0.1891	0.1971
no. of solvent molecules (total occupancies)	278 (209.9)	191 (151.7)
rmsd from ideality		
bonds (Å)	0.011	0.011
angle distances (Å)	0.032	0.029
average *B* factor (Å^2)		
main chain atoms	14.1	18.9
side chain atoms	19.6	23.9
inhibitor	10.9	15.4
solvent	28.1	36.8
relative occupancy of inhibitor	0.64/0.36	0.73/0.27

Processing was only partially inhibited by LPV (Figure 4B) but was completely inhibited by DRV (Figure 4D), using both inhibitors at a concentration of 6 μM. SQV is intermediate in its inhibition of TFR-PR_{L76V}, autoprocessing being slightly better than LPV and poorer than DRV. Internal cleavages within the TFR have been shown to be less responsive to inhibition than cleavages at the TFR-PR site.[19] Thus, in the presence of LPV and SQV, some cleavage occurred at the F8−L9 bond to give the intermediate TFR^{9-56}-PR_{L76V}, but very little or no subsequent cleavage was detected at the N-terminus of the protease domain to give mature PR_{L76V}.

The L76V single mutation severely compromises viral replication in cell cultures, whereas the coexistence of another mutation, M46I, was found to increase resistance to LPV while also partially restoring the ability of the virus to replicate.[10] This presumably occurs with an increase in the stability and/or catalytic efficiency of the protease or its precursor. Unfortunately, it was not possible to isolate the mature $PR_{M46I/L76V}$ because of its rapid autoproteolysis and very poor accumulation during its expression. However, limited quantities of the precursor TFR-$PR_{M46I/L76V}$ could be obtained for comparison with TFR-PR_{L76V} under the same conditions. In the absence of inhibitors, TFR-$PR_{M46I/L76V}$ undergoes autoprocessing significantly faster (Figure 4E) than TFR-PR_{L76V}. The additional M46I mutation has no effect on inhibition by 6 μM SQV or DRV (Figure 4G,H). Interestingly, however, TFR-$PR_{M46I/L76V}$ almost completely evades inhibition (Figure 4F) under conditions where LPV inhibits processing of the single mutant TFR-PR_{L76V}. These results are consistent with the observations of Nijhuis et al.[10] and underscore the potential importance of secondary mutations for precursor processing, both by improving the intrinsic autoprocessing activity of an

otherwise compromised precursor and by decreasing its susceptibility to inhibition.

PR_{L76V}−Inhibitor Crystal Structures. Crystal structures of PR_{L76V} in complexes with DRV and SQV were determined to identify any structural changes caused by the mutation. The crystallographic data collection and refinement statistics are listed in Table 2. The crystal structures of the PR_{L76V}−DRV and PR_{L76V}−SQV complexes were refined to *R* factors of 0.14 at resolutions of 1.45 and 1.46 Å, respectively. The crystal structures had one PR dimer with residues labeled 1−99 and 1′−99′ in each crystallographic asymmetric unit in space group $P2_12_12$. DRV and SQV were observed in two alternate conformations in the active site cavity of the dimer of PR_{L76V} with relative occupancies of 0.63/0.37 and 0.73/0.27, respectively. Alternate conformations were modeled for 10 and 17 residues in the PR_{L76V}−SQV and PR_{L76V}−DRV structures, respectively. Flap residues 46, 50, and 51 exhibited alternative conformations in both subunits of the two structures. The DRV complex also exhibited alternative conformations of the side chains for Val82, Pro81′, Val82′, and I84′ in the inhibitor binding site; however, these residues showed a single conformation in the SQV complex. The structures were refined with more than 200 water molecules. The solvent included one sodium ion, two chlorides, and three acetate molecules in the DRV complex, while the SQV complex had eight glycerol molecules.

Structural Changes at the Site of Mutation. The PR_{L76V}−DRV and −SQV complexes were compared with the corresponding PR−inhibitor complexes. The PR−DRV (PDB entry 2IEN)[25] structure was determined in the same space group ($P2_12_12$) at 1.30 Å resolution. The DRV complexes shared very similar backbone conformations with a low rmsd of 0.11 Å on Cα atoms. The PR−SQV (PDB entry 2NMW)[8] structure was refined at 1.16 Å resolution in the same space group, although the unit cell dimensions differed. Hence, the SQV complexes with PR_{L76V} and PR superimposed with the larger rmsd value of 0.65 Å resulting from variations of up to 2.3 Å in residues 37−41 and 36′−45′, which are typically seen for PR complexes in different space groups.

Leu76 lies in the inner hydrophobic cluster in each subunit of the PR dimer,[38] and its side chain makes hydrophobic contacts with the side chains of Asp30, Val32, Lys45, Ile47, Val56, Gln58, and Thr74. The mutation of leucine 76 to valine gives a shorter side chain, which results in the loss of several van der Waals contacts. In the PR_{L76V}−DRV complex, hydrophobic contacts with the side chains of Asp30, Lys45, and Thr74 and one contact with Ile47 are lacking in both subunits, as shown by an interatomic distance of more than 4.2 Å (Figure 5A). Instead, the mutated Val76 forms more and closer hydrophobic interactions with the side chain of Val32, with interatomic distances of 3.8−4.0 Å rather than the longer 4.2 Å separation seen in the PR structure. Similar changes are observed in the PR_{L76V}−SQV complex, with the exception of contacts with Val32 and Val56. The side chains of Val56 and residue 76 exhibit multiple hydrophobic contacts in the PR_{L76V} complexes with both inhibitors and in the PR−DRV structure; however, the PR−SQV structure shows only a single van der Waals interaction between these residues (Figure 5B,C). Similarly, the side chains of Leu76 and Val32 show no hydrophobic contacts in the PR−SQV complex, while multiple contacts are seen in the PR_{L76V}−SQV complex and in both DRV complexes. Thus, the PR−SQV complex shows fewer internal contacts around Leu76 compared to the number around Val76 in the mutant complex, whereas similar contacts of residues 32, 56, and 76 are maintained in both DRV complexes.

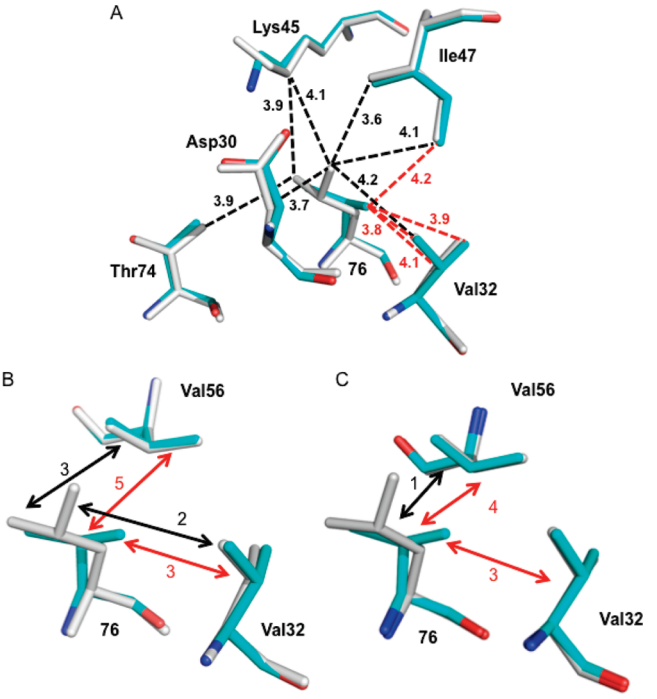

Figure 5. Hydrophobic interactions of residue 76 in the crystal structures of PR_{L76V} (cyan) and wild-type PR (gray). (A) Interactions of residue 76 in subunit A of the PR_{L76V}−DRV and PR−DRV complexes. Leu76 forms van der Waals contacts (3.6−4.2 Å) with the side chains of Asp30, Val32, Lys45, Ile47, and Thr74 (black dashed lines), while Val76 in PR_{L76V} has hydrophobic contacts with only Val32 and Ile47 (red dashed lines). Interatomic distances are given in angstroms. Neighboring residue Gln58 is not shown because it forms similar interactions with residue 76 in PR and PR_{L76V}. Val56 was omitted for the sake of clarity. (B) Interactions of residue 76 with Val32 and Val56 in the PR_{L76V}−DRV and PR−DRV complexes. (C) Interactions of residue 76 with Val32 and Val56 in the PR_{L76V}−SQV and PR−SQV complexes. In panels B and C, the number of hydrophobic contacts between the side chains is indicated by black (with Leu76) and red (with Val76) arrows.

The decrease in the number of internal van der Waals interactions is correlated with the lower stability of the mutant relative to the wild-type enzyme described in the previous section. In contrast to other mutants exhibiting lower stability such as PR_{L24I}, PR_{I50V}, and PR_{F53L},[9,39] however, no significant changes were seen at the dimer interface of the mutant structures. Therefore, the major molecular change associated with the significantly lower stability of PR_{L76V} is the loss of internal hydrophobic contacts characteristic of Leu76. This loss of hydrophobic contacts at the mutated residue stands in strong contrast to the minimal changes reported for the majority of single mutants.[9,40] For example, our recent analysis of six mutants with single substitutions of residues in the hydrophobic clusters showed small structural adjustments that tended to conserve the hydrophobic interactions.[40] Hence, the major loss of internal hydrophobic contacts for Val76 in PR_{L76V}, coupled with the reduced stability that is offset by secondary mutations, exemplifies a distinct mechanism for drug resistance.

Protease−Inhibitor Interactions. In the crystal structure of the PR_{L76V}−DRV complex, the inhibitor is observed in two orientations bound within the active site cavity by a set of hydrogen bonds, which are similar to those in the PR−DRV

dx.doi.org/10.1021/bi200033z |*Biochemistry* 2011, 50, 4786–4795

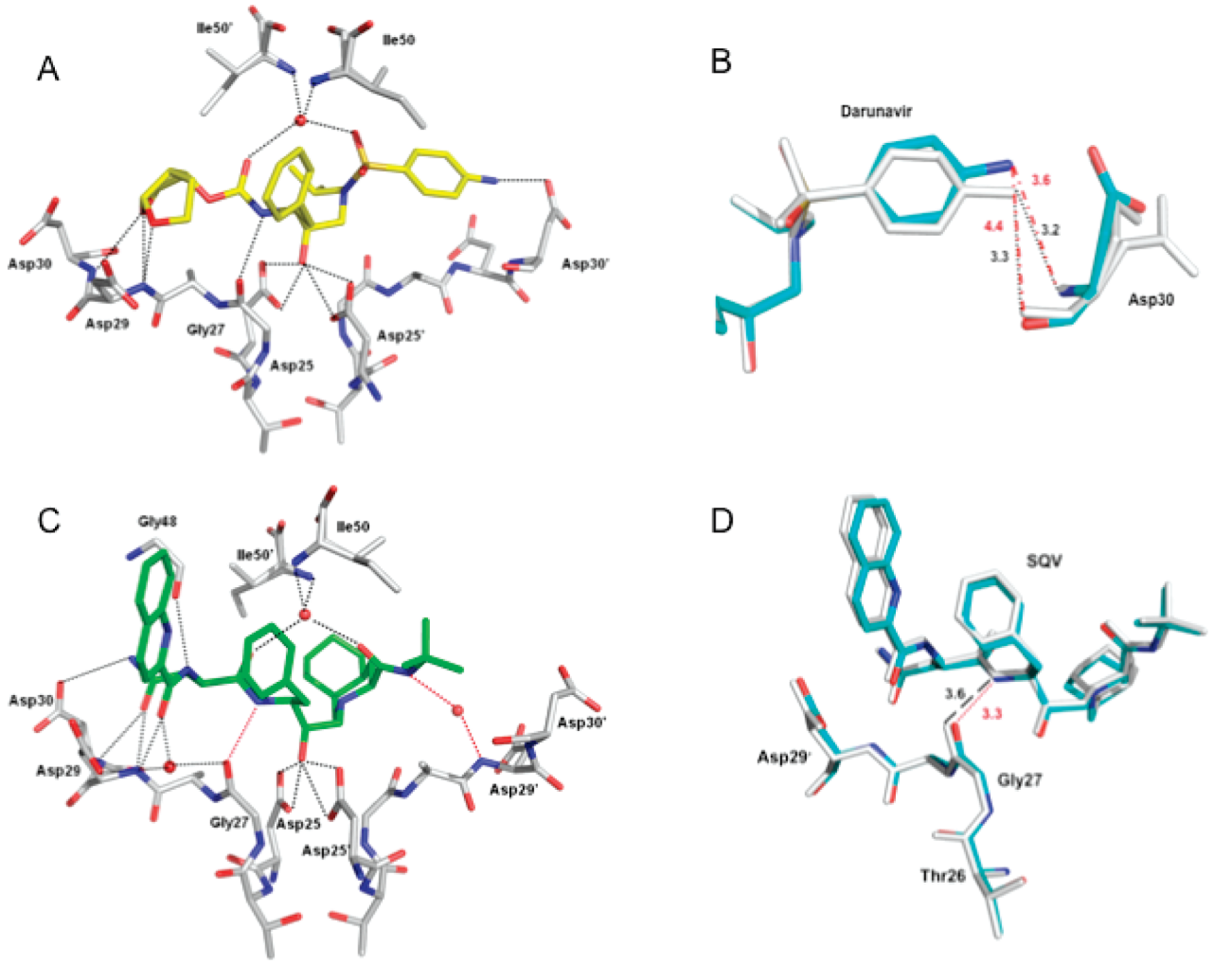

Figure 6. Protease−inhibitor hydrogen bond interactions. Hydrogen bonds are represented as dotted lines. Water molecules are represented as red spheres. (A) Hydrogen bond interactions of PR_{L76V} with the major conformation of DRV (yellow). (B) Superposition of the PR_{L76V}−DRV (cyan bonds) and PR−DRV (gray bonds) complexes showing PR_{L76V} has fewer hydrogen bond interactions with the aniline group of DRV. The side chain of Asp30 has two alternate conformations in the PR−DRV structure. Interatomic distances are given in angstroms with black dotted lines indicating the hydrogen bond interactions in the wild-type complex and red dashed lines showing the larger interatomic separation in the mutant. (C) PR_{L76V} hydrogen bond interactions with the major conformation of SQV (green). The red dotted lines indicate the new hydrogen bond interactions formed by SQV in PR_{L76V} relative to the PR−SQV complex. (D) Superposition of the PR_{L76V}−SQV (cyan bonds) and PR−SQV (gray bonds) complexes showing the improved interaction of SQV with PR_{L76V} arising from only slight structural changes. The red dotted line indicates the new hydrogen bond interaction in the mutant, and the black dashed line shows the larger interatomic separation in the wild type SQV complex.

complex.[25] Both orientations of DRV show similar hydrogen bond interactions with PR_{L76V}. DRV forms four hydrogen bonds with the main chain atoms of Gly27′, Asp29′, and Asp30′ and five hydrogen bonds with the side chain atoms of Asp25/Asp25′ and Asp30 of PR_{L76V} (Figure 6A). The water-mediated hydrogen bonds between Ile50 or Ile50′ and DRV are conserved in the majority of crystal structures of PR and its mutants with inhibitors and substrates. Compared with the wild-type complex, DRV shows weaker interactions with the main chain of Asp30, which is associated with the shift of the aniline group of DRV away from Asp30 of PR_{L76V} (Figure 6B). The interatomic distance representing a hydrogen bond between the aniline amino group of DRV and the amide nitrogen of Asp30 in the PR−DRV complex increases from 3.2 to 3.6 Å in the A subunit of the PR_{L76V}−DRV complex, while the interatomic distance between the DRV amino group and the carbonyl oxygen of Asp30 increases from 3.3 to 4.4 Å, indicating the loss of a hydrogen bond in the PR_{L76V} mutant. These changes may correlate with the loss of internal van der Waals contacts of Val76, especially those with Asp30, relative to those of the wild-type Leu76.

SQV is bound at the active site in two pseudosymmetric orientations in the PR_{L76V}−SQV complex. The major conformation of SQV forms nine direct hydrogen bond interactions and four water-mediated hydrogen bonds with PR_{L76V} (Figure 6C). The mutant exhibits one improved direct and one more water-mediated interaction with SQV as compared with those in the wild-type complex. Notably, a 3.3 Å hydrogen bond interaction is formed between the carbonyl oxygen of Gly27 and the amide of SQV compared to the very weak 3.6 Å interaction observed in the wild-type complex (Figure 6D). The conserved water-mediated hydrogen bonds are seen between Ile50 or Ile50′ and SQV, and another water-mediated interaction is conserved in reported high-resolution crystal structures of PR and its mutants with SQV.[8] Compared with the PR−SQV crystal structure, one more

dx.doi.org/10.1021/bi200033z |*Biochemistry* 2011, 50, 4786–4795

water-mediated hydrogen bond is observed between SQV and the amide of Asp29 in PR_{L76V}. No water was visible at the equivalent position in the wild-type structure; however, the observation of ordered solvent molecules partly depends on the crystallization conditions, quality, and resolution of the diffraction data. Overall, SQV has slightly improved hydrogen bond interactions with PR_{L76V} relative to those with the wild-type PR, suggesting that the mutant may retain high binding affinity for this inhibitor.

Implications for Drug Resistance. The structural changes in the PR_{L76V}−inhibitor complexes suggest the molecular basis for the lowered stability of this mutant and slower autoprocessing of its precursor. The diminished hydrophobic interactions of Val76 can directly perturb the interactions of DRV with Asp30, although no direct effect on the SQV interactions was seen. Also, the mutation is likely to perturb the flaps through loss of contacts between residue 76 and flap residues Lys45 and Ile47. Movement of the flaps is required for binding of substrate and release of products.[39] Interflap contacts also contribute to the dimer interface, so that destabilization of the flaps will likely contribute to the higher dimer dissociation constant of PR_{L76V} and its increased susceptibility to thermally induced and urea-induced denaturation. Consequently, precursor processing, formation of the mature dimer, and drug resistance depend on maintaining the correct flap conformations and their contacts with internal hydrophobic residues like Leu76.

The properties of this mutant are discussed in relation to the interactions of the nine clinical inhibitors to understand why the L76V mutation is associated with increased resistance to some drugs while retaining effective binding affinity for other clinical inhibitors. DRV forms no direct hydrogen bonds with flap residues, suggesting that its binding may allow changes in flap conformation (Figure 6A). In contrast, SQV forms a hydrogen bond with the carbonyl oxygen of Gly48 in the flap, which suggests SQV binding may restrict such conformational changes (Figure 6C). This analysis of the PR_{L76V} crystal structures and other PR complexes sheds light on the opposing clinical responses of this mutant to different drugs.[10,11,13] The L76V mutation is associated with resistance to the inhibitors LPV, DRV, APV, and IDV, which form hydrogen bond interactions with Gly27, Asp29, and/or Asp30 near the catalytic Asp25, as well as the conserved water-mediated interactions with Ile50 and Ile50′.[25,33,40,41] On the other hand, inhibitors ATV, SQV, and TPV, for which mutants containing L76V exhibit increased susceptibility, all form direct or water-mediated hydrogen bond interactions with Gly48, while TPV is unique in forming direct, instead of water-mediated, hydrogen bonds with the amides of Ile50 and Ile50′.[33] NFV is the only exception with no direct flap interactions;[42] however, susceptibility to NFV is less strongly associated with the L76V mutation compared to other drugs.[11,12]

The observed structural changes provide insight into the effects of combining the L76V and M46I mutations, which has been reported to contribute strongly to the competence of the virus to replicate and its clinical resistance to LPV.[10] Analysis of the wild-type PR crystal structures suggests that the P2 group of LPV is unusual in forming multiple close hydrophobic contacts with Ile47, whereas DRV and SQV show only one or two hydrophobic contacts with Ile47. Thus, altered contacts with flap residues 45 and 47 associated with the L76V mutation may partially weaken the binding affinity of LPV and contribute to resistance to this drug while having less effect on the response to other drugs. Residues 46 and 76 have no direct contacts in the dimer structure, because residue 76 is part of the internal hydrophobic cluster, while the side chain of residue 46 points away from the protein surface of the flexible flap. Instead, Leu76 contacts the side chains of Lys45 and Ile47 on either side of Met46. In PR_{L76V}, Lys45 and Ile47 exhibit diminished interactions with Val76, suggesting that the M46I mutation may indirectly compensate for the destabilizing effects of the L76V mutation. Notably, although PR_{L76V} shows a much slower rate of autoprocessing of its precursor relative to the wild type, in agreement with reported defective viral replication,[10] the rate is increased upon introduction of the M46I mutation (Figure 4D). Furthermore, the presence of both mutations significantly restores autoprocessing capability in the presence of LPV, although inhibition by DRV is retained. These results are consistent with previous data on viral replication in cell cultures[10] and suggest that investigating effects on precursor processing and its inhibition will provide a useful approach, which is complementary to studies of interactions of the inhibitor with the mature protease, for understanding the role and interactions of multiple mutations in drug resistance.

AUTHOR INFORMATION

Corresponding Authors

*I.T.W.: Department of Biology, Georgia State University, P.O. Box 4010, Atlanta, GA 30302-4010; phone, (404) 413-5411; fax, (404) 413-5301; e-mail, iweber@gsu.edu. J.M.L.: Building 5, Room B2-29, LCP, NIDDK, NIH, Bethesda, MD 20892-0520; phone, (301) 594-3122; fax, (301) 480-4001; e-mail, johnl@intra.niddk.nih.gov.

Author Contributions

J.M.L. and Y.Z. contributed equally to this work.

Funding Sources

This research was supported, in whole or in part, by National Institutes of Health (NIH) Grant GM062920, the Intramural Research Program of the National Institute of Diabetes and Digestive and Kidney Diseases, and Intramural AIDS-Targeted Antiviral Program of the Office of the Director, NIH.

ACKNOWLEDGMENT

We thank Annie Aniana for technical assistance and the staff at SER-CAT beamline at the Advanced Photon Source for assistance during X-ray data collection. Use of the Advanced Photon Source was supported by the U.S. Department of Energy, Office of Science, Office of Basic Energy Sciences, under Contract W-31-109-Eng-38. DRV, LPV, and SQV were obtained through the NIH AIDS Research and Reference Reagent Program, Division of AIDS, National Institute of Allergy and Infectious Diseases, NIH.

ABBREVIATIONS

HIV-1, human immunodeficiency virus type 1; PR, pseudo-wild-type HIV-1 protease optimized for structural and biochemical studies by introduction of the Q7K, L33I, L63I, C67A, and C95A mutations; PR_{L76V}, PR with the L76V mutation; DRV, darunavir; SQV, saquinavir; LPV, lopinavir; Nle, norleucine; DMSO, dimethyl sulfoxide; rmsd, root-mean-square deviation; DSC, differential scanning calorimetry; ITC, isothermal titration calorimetry; RPB,

H-Arg-Val-Leu-(r)-Phe-Glu-Ala-Nle-NH_2 inhibitor with a reduced peptide bond at position r.

REFERENCES

(1) Turner, B. F., and Summers, M. F. (1999) Structural biology of HIV. *J. Mol. Biol. 285*, 1–32.

(2) Cherry, E., and Wainberg, M. A. (2002) The Structure and Biology of HIV 1. In *The human Immunodeficiency Virus: Biology, Immunology, and Therapy* (Emini, E. A., Ed.) pp 1−43, Princeton University Press, Princeton, NJ.

(3) Louis, J. M., Weber, I. T., Tözsér, J., Clore, G. M., and Gronenborn, A. M. (2000) HIV-1 protease: Maturation, enzyme specificity, and drug resistance. *Adv. Pharmacol. 49*, 111–146.

(4) Brik, A., and Wong, C. H. (2003) HIV-1 protease: Mechanism and drug discovery. *Org. Biomol. Chem. 1*, 5–14.

(5) Weber, I. T., and Agniswamy, J. (2009) HIV-1 protease: Structural perspectives on drug resistance. *Viruses 1*, 1110–1136.

(6) Weber, I. T. (1990) Comparison of the crystal structures and intersubunit interactions of human immunodeficiency and Rous sarcoma virus proteases. *J. Biol. Chem. 265*, 10492–10496.

(7) Johnson, V. A., Brun-Vézinet, F., Clotet, B., Günthard, H. F., Kuritzkes, D. R., Pillay, D., Schapiro, J. M., and Richman, D. D. (2009) Update of the drug resistance mutations in HIV-1: December 2009. *Top. HIV Med. 17*, 138–145.

(8) Tie, Y., Kovalevsky, A. Y., Boross, P., Wang, Y. F., Ghosh, A. K., Tozser, J., Harrison, R. W., and Weber, I. T. (2007) Atomic resolution crystal structures of HIV-1 protease and mutants V82A and I84V with saquinavir. *Proteins: Struct., Funct., Bioinf. 67*, 232–242.

(9) Liu, F., Boross, P. I., Wang, Y. F., Tozser, J., Louis, J. M., Harrison, R. W., and Weber, I. T. (2005) Kinetic, stability, and structural changes in high-resolution crystal structures of HIV-1 protease with drug-resistant mutations L24I, I50V, and G73S. *J. Mol. Biol. 354*, 789–800.

(10) Nijhuis, M., Wensing, A. M. J., Bierman, W. F. W., de Jong, D., Kagan, R., Fun, A., Jaspers, C. A. J. J., Schurink, K. A. M., van Agtmael, M. A., and Boucher, C. A. B. (2009) Failure of treatment with first line lopinavir boosted with ritonavir can be explained by novel resistance pathways with protease mutation 76V. *J. Infect. Dis. 200*, 698–709.

(11) Young, T. P., Parkin, N. T., Stawiski, E., Pilot-Matias, T., Trinh, R., Kempf, D. J., and Norton, M. (2010) Prevalence, Mutation Patterns and Effects on Protease Inhibitor Susceptibility of the L76V Mutation in HIV-1 Protease. *Antimicrob. Agents Chemother. 54*, 4903–4906.

(12) Rhee, S. Y., Taylor, J., Fessel, W. J., Kaufman, D., Towner, W., Troia, P., Ruane, P., Hellinger, J., Shirvani, V., Zolopa, A., and Shafer, R. W. (2010) HIV-1 protease mutations and protease inhibitor cross-resistance. *Antimicrob. Agents Chemother. 54*, 4253–4261.

(13) Mueller, S. M., Daeumer, M., Kaiser, R., Walter, H., Colonno, R., and Korn, K. (2004) Susceptibility to saquinavir and atazanavir in highly protease inhibitor (PI) resistant HIV-1 is caused by lopinavir-induced drug resistance mutation L76V. *Antiviral Ther. 9*, S44.

(14) Vermeiren, H., Van Craenenbroeck, E., Alen, P., Bacheler, L., Picchio, G., and Lecocq, P. (2007) Prediction of HIV-1 drug susceptibility phenotype from the viral genotype using linear regression modeling. *J. Virol. Methods 145*, 47–55.

(15) Tartaglia, A., Saracino, A., Monno, L., Tinelli, C., and Angarano, G. (2009) Both a Protective and a Deleterious Role for the L76V Mutation. *Antimicrob. Agents Chemother. 53*, 1724–1725.

(16) Louis, J. M., Clore, G. M., and Gronenborn, A. M. (1999) Autoprocessing of HIV-1 protease is tightly coupled to protein folding. *Nat. Struct. Biol. 6*, 868–875.

(17) Wondrak, E. M., and Louis, J. M. (1996) Influence of flanking sequences on the dimer stability of human immunodeficiency virus type 1 protease. *Biochemistry 35*, 12957–12962.

(18) Ishima, R., Torchia, D. A., and Louis, J. M. (2007) Mutational and structural studies aimed at characterizing the monomer of HIV-1 protease and its precursor. *J. Biol. Chem. 282*, 17190–17199.

(19) Sayer, J. M., Agniswamy, J., Weber, I. T., and Louis, J. M. (2010) Autocatalytic maturation, physical/chemical properties and crystal structure of group N HIV 1 protease: Relevance to drug resistance. *Protein Sci. 19*, 2055–2072.

(20) Liu, F., Kovalevsky, A. Y., Tie, Y., Ghosh, A. K., Harrison, R. W., and Weber, I. T. (2008) Effect of flap mutations on structure of HIV-1 protease and inhibition by saquinavir and darunavir. *J. Mol. Biol. 381*, 102–115.

(21) Mahalingam, B., Louis, J. M., Reed, C. C., Adomat, J. M., Krouse, J., Wang, Y. F., Harrison, R. W., and Weber, I. T. (1999) Structural and kinetic analysis of drug resistant mutants of HIV-1 protease. *FEBS J. 263*, 238–244.

(22) Sayer, J. M., Liu, F., Ishima, R., Weber, I. T., and Louis, J. M. (2008) Effect of the active site D25N mutation on the structure, stability, and ligand binding of the mature HIV-1 protease. *J. Biol. Chem. 283*, 13459–13470.

(23) Otwinowski, Z., and Minor, W. (1997) Processing of X-ray diffraction data collected in oscillation mode. *Methods Enzymol. 267*, 307–326.

(24) Vagin, A., and Teplyakov, A. (1997) MOLREP: An automated program for molecular replacement. *J. Appl. Crystallogr. 30*, 1022–1025.

(25) Tie, Y., Boross, P. I., Wang, Y. F., Gaddis, L., Hussain, A. K., Leshchenko, S., Ghosh, A. K., Louis, J. M., Harrison, R. W., and Weber, I. T. (2004) High resolution crystal structures of HIV-1 protease with a potent non-peptide inhibitor (UIC-94017) active against multi-drug-resistant clinical strains. *J. Mol. Biol. 338*, 341–352.

(26) Sheldrick, G. M., and Schneider, T. R. (1997) SHELXL: High-resolution refinement. *Methods Enzymol. 277*, 319–343.

(27) Emsley, P., and Cowtan, K. (2004) Coot: Model-Building Tools for Molecular Graphics. *Acta Crystallogr. D60*, 2126–2132.

(28) DeLano, W. L. (2002) *The PyMOL Molecular Graphics System*, DeLano Scientific, San Carlos, CA.

(29) Louis, J. M., Ishima, R., Torchia, D. A., and Weber, I. T. (2007) HIV-1 protease: Structure, dynamics, and inhibition. *Adv. Pharmacol. 55*, 261–298.

(30) Sayer, J. M., and Louis, J. M. (2009) Interactions of different inhibitors with active site aspartyl residues of HIV 1 protease and possible relevance to pepsin. *Proteins: Struct., Funct., Bioinf. 75*, 556–568.

(31) Yanchunas, J., Jr., Langley, D. R., Tao, L., Rose, R. E., Friborg, J., Colonno, R. J., and Doyle, M. L. (2005) Molecular basis for increased susceptibility of isolates with atazanavir resistance-conferring substitution I50L to other protease inhibitors. *Antimicrob. Agents Chemother. 49*, 3825–3832.

(32) Todd, M. J., Luque, I., Velázquez-Campoy, A., and Freire, E. (2000) Thermodynamic basis of resistance to HIV-1 protease inhibition: Calorimetric analysis of the V82F/I84V active site resistant mutant. *Biochemistry 39*, 11876–11883.

(33) Muzammil, S., Armstrong, A. A., Kang, L. W., Jakalian, A., Bonneau, P. R., Schmelmer, V., Amzel, L. M., and Freire, E. (2007) Unique thermodynamic response of tipranavir to human immunodeficiency virus type 1 protease drug resistance mutations. *J. Virol. 81*, 5144–5154.

(34) King, N. M., Prabu-Jeyabalan, M., Nalivaika, E. A., Wigerinck, P., de Béthune, M. P., and Schiffer, C. A. (2004) Structural and thermodynamic basis for the binding of TMC114, a next-generation human immunodeficiency virus type 1 protease inhibitor. *J. Virol. 78*, 12012–12021.

(35) Brower, E. T., Bacha, U. M., Kawasaki, Y., and Freire, E. (2008) Inhibition of HIV-2 protease by HIV-1 protease inhibitors in clinical use. *Chem. Biol. Drug Des. 71*, 298–305.

(36) Mitsuya, Y., Liu, T. F., Rhee, S. Y., Fessel, W. J., and Shafer, R. W. (2007) Prevalence of darunavir resistance and associated mutations: Patterns of occurrence and association with past treatment. *J. Infect. Dis. 196*, 1177–1179.

(37) Louis, J. M., Wondrak, E. M., Kimmel, A. R., Wingfield, P. T., and Nashed, N. T. (1999) Proteolytic processing of HIV-1 protease precursor, kinetics and mechanism. *J. Biol. Chem. 274*, 23437–23442.

(38) Ishima, R., Louis, J. M., and Torchia, D. A. (2001) Characterization of two hydrophobic methyl clusters in HIV-1 protease by NMR spin relaxation in solution. *J. Mol. Biol. 305*, 515–521.

(39) Liu, F., Kovalevsky, A. Y., Louis, J. M., Boross, P. I., Wang, Y. F., Harrison, R. W., and Weber, I. T. (2006) Mechanism of drug resistance revealed by the crystal structure of the unliganded HIV-1 protease with F53L mutation. *J. Mol. Biol. 358*, 1191–1199.

(40) Shen, C. H., Wang, Y. F., Kovalevsky, A. Y., Harrison, R. W., and Weber, I. T. (2010) Amprenavir complexes with HIV-1 protease and its drug-resistant mutants altering hydrophobic clusters. *FEBS J. 277*, 3699–3714.

(41) Mahalingam, B., Wang, Y. F., Boross, P. I., Tozser, J., Louis, J. M., Harrison, R. W., and Weber, I. T. (2004) Crystal structures of HIV protease V82A and L90M mutants reveal changes in the indinavir-binding site. *Eur. J. Biochem. 271*, 1516–1524.

(42) Kaldor, S. W., Kalish, V. J., Davies, J. F., Shetty, B. V., Fritz, J. E., Appelt, K., Burgess, J. A., Campanale, K. M., Chirgadze, N. Y., Clawson, D. K., Dressman, B. A., Hatch, S. D., Khalil, D. A., Kosa, M. B., Lubbehusen, P. P., Muesing, M. A., Patick, A. K., Reich, S. H., Su, K. S., and Tatlock, J. H. (1997) Viracept (nelfinavir mesylate, AG1343): A potent, orally bioavailable inhibitor of HIV-1 protease. *J. Med. Chem. 40*, 3979–3985.